

NUMERICAL EVALUATION OF COMPRESSION LOCALIZATION OF CONCRETE UNDER STEEL TUBE CONFINEMENT

Rodolfo Mendoza Jr.^{*1}, Yoshihito Yamamoto^{*2}, Hikaru Nakamura^{*3} and Taito Miura^{*4}

ABSTRACT

The effect of increasing steel ratio and slenderness on the length of compressive localization zone in concrete under steel tube confinement is investigated. The analysis is performed using the newly developed coupled Rigid Body Spring Model and nonlinear shell FEM which represents concrete and steel, respectively, in a steel tube confined concrete member. It was found that the compressive behavior of steel-tube confined concrete is also localized, and the length of localization damage tends to increase with increasing steel ratio. Evaluation of the development of lateral stresses in the steel tube shows that when the confining pressure provided by the steel tube is low, the steel tube is unable to restrain the lateral expansion of concrete, thus localization occurs. However, when sufficient confining pressure is provided by the steel tube, the damage is forced to propagate longitudinally along the length of the member causing a more or less uniform damage.

Keywords: localization, confinement, RBSM, nonlinear shell, steel-tube confined concrete

1. INTRODUCTION

The flexural ductility and strength provided by a confinement are influenced by the strength enhancement provided by the confining material (e.g., level of confining pressure) and the slope of the descending branch of the concrete stress-strain curve [1]. The slope of the descending branch of the concrete stress-strain curve, on the other hand, is influenced by the localization of concrete in compression. This compression localization in concrete occurs when the axial deformation of concrete concentrates (localizes) in a small region when subjected to compressive load. The phenomenon is well-recognized and has been shown repeatedly through experiments by various researchers (e.g., Nakamura and Higai [2]). The major consequence, in particular to ductility, is that larger specimens or members failing in a compressive mode show less ductility in the post-peak region than smaller specimens [3]. A solution to reduce or even eliminate the effect of this mechanism is to laterally confine concrete.

Caner and Bazant [4] investigated the amount of confinement (expressed in terms of steel ratio) needed to suppress the softening of the concrete stress-strain curve. They concluded that a steel ratio of 14% is required to fully suppress the softening while if a mild softening is allowed, a steel ratio of at least 8% may be used. These recommendations were derived based on combined experimental data from tube squash test and FEM analysis with Microplane model in which the effect of the length of compressive fracture (damage)

zone was not directly studied. It was found, however, through the works of Wu and Wei [5] from test results of FRP-confined concrete columns that the length of compressive fracture zone tends to increase with increasing level of confinement. This suggests that for a given confining pressure, the length of compressive fracture zone may engulf the entire height of the member and the localization of damage in concrete will not be apparent. However, when the member height becomes greater than the localization length, localization of damage will become visible. This means that the amount of steel ratio or confinement needed to suppress localization is a function of the slenderness of the columns. To date, the mechanism behind this observation has not yet been clarified.

This paper aims to understand this observation by evaluating the effect of increasing steel ratio and column slenderness in the compressive localization of concrete under steel tube confinement. To achieve this, a newly developed coupled numerical model is introduced which combines the use of Rigid Body Spring Model and nonlinear shell FEM. The RBSM is selected to model concrete as it has been proven to provide an accurate representation of concrete's compressive behavior, which includes strain softening and compression localization (see Yamamoto et al. [6]). For steel tube modeling, a geometrically nonlinear shell is used in order to capture large displacement and rotation effects. To provide a confidence in the proposed model, a validation of RBSM and the coupled RBSM-shell model is first presented through comparison with published test data. The onset of

*1 Ph.D. student, Dept. of Civil Engineering, Nagoya University, JCI Member

*2 Associate Professor, Dept. of Civil Engineering, Nagoya University, JCI Member

*3 Professor, Dept. of Civil Engineering, Nagoya University, JCI Member

*4 Assistant Professor, Dept. of Civil Engineering, Nagoya University, JCI Member

interaction between concrete and steel in a concrete-filled steel tube member loaded on both concrete and steel section has been explained by several authors. The interaction of the two materials for the case where only the concrete section is axially loaded and the steel tube is used primarily for confinement, however, has never been fully discussed. Using the same test data used in the validation, the interaction of concrete and steel under passive confinement condition is evaluated by studying the progress of cracks and local axial strains in concrete, and stress development and yielding of steel tube. Finally, analysis results of steel-tube confined concrete columns with steel ratio of $\rho_s = 0.9, 1.8, 8.0,$ and 14.8% , and with varying height-to-diameter (H/D) ratio of 2, 3, and 4 are presented. The effect of these investigated variables in the length of compression fracture or damage zone of concrete under steel tube confinement is discussed.

2. NUMERICAL MODELING

The modeling of steel-tube confined concrete is performed using the newly coupled RBSM and nonlinear shell FEM. The coupled model highlights its capability in capturing the localization of damage in concrete under steel tube confinement, which is one of the important features of the 3D RBSM model developed by Yamamoto et al. [6]. The RBSM model is combined with a geometrically nonlinear shell FEM model capable of capturing local steel tube buckling. The representation of concrete and steel tube using the said model is shown in Fig. 1. The key to capturing the strain-softening and localization behavior of concrete using RBSM lies in the use of appropriate constitutive models. The constitutive models adopted for concrete in the proposed coupled model are based on the work of Yamamoto et al. [6]. A detailed account of these models can be found in Yamamoto et al. [6], and summary in Mendoza et al. [7].

A description of the geometry and displacement equations of the developed nonlinear shell finite element is given in Mendoza et al. [7]. The four-node isoparametric element consists of five degrees-of-freedom at each node. The shear locking problem commonly present in shell elements is solved using a selective reduced integration scheme. Material

modeling of steel is linear isotropic hardening with failure criterion based on J_2 plasticity. The performance of the developed shell program has been verified with benchmark models for geometrically nonlinear shell with good performance and this can be found in Mendoza et al. [8].

The interaction between concrete and steel is modeled using discrete interface element pre-assigned on RBSM element surfaces that are in contact with shell elements (see Fig. 1).

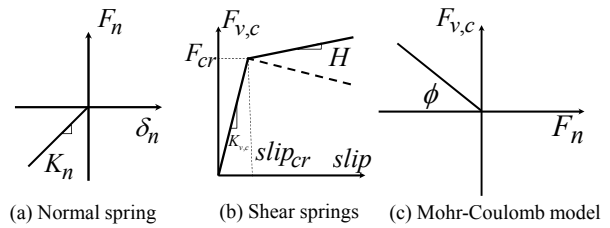


Fig. 2 Constitutive models for interface elements between RBSM and shell

To relate the displacements at contact points to the shell nodes, an inverse mapping algorithm was introduced. A discussion on this approach is found in Mendoza et al. [7]. The interface elements consist of a set of one normal and two shear springs. Constitutive models for normal and shear springs including a representation of the Mohr-Coulomb failure criterion are shown in Fig. 2. The behavior of the normal spring is assumed to be linear, that is, with increasing contact, the normal force increases. However, under tension case, the model allows the separation of concrete and steel, and therefore, the force in the normal spring becomes zero. For the case of the shear springs, when the contact in the normal spring is compression (increasing pressure), the friction between the two materials increases and thus the forces in the shear springs (i.e. hardening occurs). When the force in the normal spring is under tension (separation of steel and concrete), the forces in the shear springs gradually reduces (softening) until the value becomes zero. For the detailed discussion on the numerical formulation and material modeling of the interface elements adopted in this study, the reader is referred to Mendoza et al. [8].

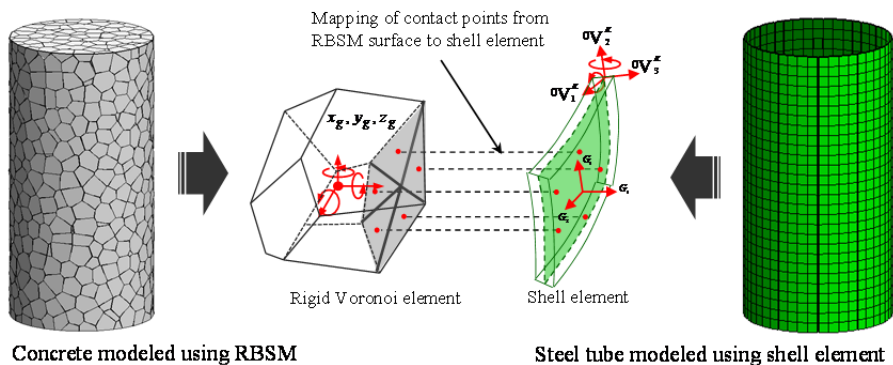


Fig. 1 The RBSM-Shell Model

3. MODEL VALIDATION

To provide a confidence on the use of the proposed model, a validation is performed by simulating the triaxial and steel-tube confined concrete test data of Lahlou et al. [9]. The test was performed on $54\phi \times 118$ mm cylindrical specimens with three different concrete strengths. Here, we present only the test results for concrete with a strength of 47 MPa. The thicknesses of steel tubes used in this validation are 0.5 mm and 1.27 mm with steel yield strength of 450 MPa. In the test, the equivalent confining pressure provided by these steel tube using equilibrium equation (thin-tube theory) were determined to be 7.6 MPa and 22 MPa, respectively. These equivalent confining pressures were then used to test the same strength of concrete under triaxial (active) confinement using a Hoek triaxial cell.

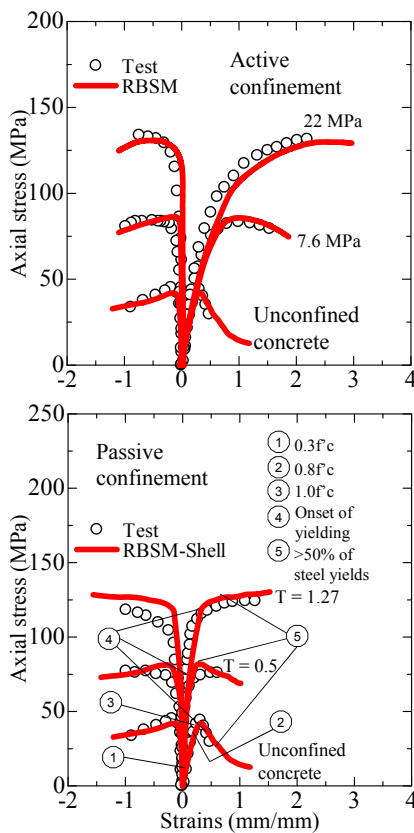


Fig. 3 Active and passive confinement validation of RBSM and coupled RBSM-shell FEM model

Axial displacements in the experiments were measured using displacement transducers and the axial strains were determined by dividing the axial displacements by the length of the specimens. Lateral strains were measured by strain gauges attached to the surface of concrete and steel tube specimens. In the simulation, the concrete was modeled using an input mesh size of 8 mm. The macroscopic material properties of concrete were used as input values for the RBSM model parameters (see [6, 7]). For the steel tube, the elements size was selected to be 5 mm. In the analysis, top and bottom plates were used to support the specimens which are assumed to be fixed. The axial load was

applied using displacement control scheme while for the triaxial simulation; the lateral pressure was applied directly to the specimens. The axial strains were measured by dividing the applied displacement with the length of the specimens. For the lateral strains, in triaxial simulation, the lateral strain was calculated by subtracting the lateral displacements at two opposite points at mid-section of the specimen and dividing this value by the diameter. For the steel tube confined concrete test, the lateral strains are the Green-Lagrange strains from the shell element output.

The comparisons between test and simulation results are presented in Fig. 3. To see the strength and ductility increase due to confinement, the result for unconfined concrete is also presented. From the active confinement results, it is clear that the RBSM can well-represent the behavior of concrete under active confinement. The simulation results fit perfectly with the test results and the simulation is able to predict quite accurately both the strength and lateral expansion of concrete. The unconfined behavior of concrete is also well-represented by RBSM. For the comparison of passive confinement test, the coupled RBSM-shell also showed an excellent performance. The model is able to represent the increase in confinement provided by the increase in steel tube thickness. Also, the predicted lateral strains obtained from shell element output can be generally considered reasonable although the predicted peak loads at peak strains are slightly overestimated. Overall, the presented validations confirm the applicability of RBSM and the proposed coupled RBSM-shell model in studying the behavior of concrete under confinement. It is important to mention that none of the test data have been used in the calibration of the model. Other validations performed to evaluate the performance of the coupled RBSM-shell model can be found in Mendoza et al. [7-8].

4. INTERACTION OF CONCRETE AND STEEL TUBE UNDER PASSIVE CONFINEMENT

It is desirable to understand how the interaction between concrete and steel develops stresses in the steel tube, and how the steel tube improves the behavior of concrete through passive confinement. The following discusses the progress in which the interaction between concrete and steel initiates. Fig. 4 shows the simulations results for the test presented in the validation section which includes the idealized cracks and calculated local axial strains in concrete, and the stresses and equivalent plastic strains in the steel tube. The idealized cracks are based on the 1/4 model shown in Fig. 4 which represent the tensile stress of RBSM normal spring. The local axial strains in RBSM are determined by calculating the relative displacements at pre-defined evaluation points (20 mm interval) and dividing this value by the initial distance between two adjacent points. The longitudinal stress in the steel tubes is represented by stress σ_{22} and lateral stress σ_{11} . To monitor the progress of yielding, the equivalent plastic strain (ϵ_{eq}) value was used to represent yielding

which happens when the value is greater than zero. The results presented are at stress levels indicated in Fig. 3. At point 1, the local axial strains in unconfined concrete showed higher values compared to confined concrete. At this stage, idealized cracks in concrete for all cases reach the first stage of post-peak tensile stress. More cracks can be observed for unconfined concrete. Longitudinal stress is visible in the steel tube and small lateral stress develops. At point 2, axial strain in unconfined concrete increases while for confined concrete, a slight increase in axial strains can be observed. Longitudinal stress in the steel tube increases (maximum near the bottom) and lateral stress starts to increase. At point 3, the idealized cracks in the unconfined concrete reach the second stage of the 1/4 model (which denotes an increase in cracking). The local axial strain has also increased substantially compared to confined concrete. At this stage, lateral stress in steel tube has increased. At point 4, the tensile stress of RBSM normal spring drops to zero for unconfined concrete and the local axial strains further increased. The idealized cracks for confined concrete reach the second stage of the 1/4 model and the axial strains start to concentrate at mid-height. For thicker steel tube, however, the local axial strains are fairly distributed compared with the specimen with a thin tube. This point also corresponds to the onset of

yielding in the steel tube. At point 5, the idealized cracks in unconfined concrete reach the failure value and the axial strain considerably increased and localized. The local axial strain for confined concrete with thin tube tends to concentrate near mid-height, while that for the thick case is relatively distributed. At this point, more than 50% of the cross-section has yielded. From the presented results, it can be concluded that the interaction between concrete and steel in passive confinement case occurs at lower axial strain (at almost the onset of loading). The lateral contact increases significantly when concrete reaches its unconfined strength. Yielding of steel in thin tube occurs at lower axial strain as compared to a specimen with a thick tube. Yielding initiates locally and propagates along the length of the member. Results also show that longitudinal stresses develop in the steel tube due to interface friction (bond). This is consistent with those observed in the test (e.g., [10]). This longitudinal stresses are higher near the bottom of the section and lower at the top of the section. This observation can be compared to the longitudinal stresses that develop under a push-out test of concrete stubs where only concrete is axially pushed [11]. Due to this, at some locations, the yielding of steel tube occurs prior to the lateral stresses reach a yield value due to the presence of compressive longitudinal stress.

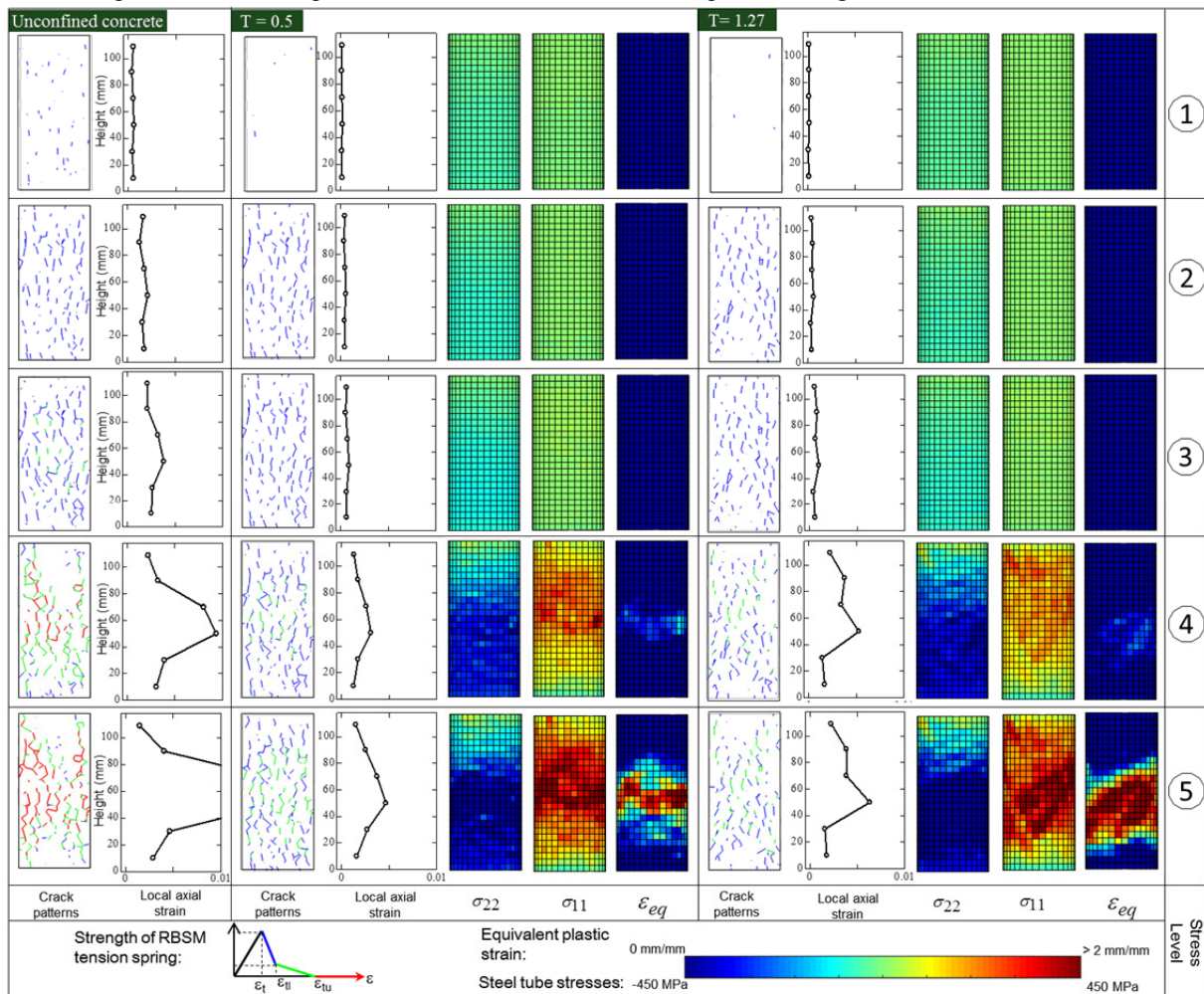


Fig. 4 Progress of concrete-steel interaction under passive confinement

In general, the effect of confinement to concrete is clear, that is, it delays the propagation of cracks in concrete and thus the strength and ductility of concrete are improved. Depending on the level of confinement, localization of deformation may occur and this will be investigated in the succeeding section.

5. LENGTH OF COMPRESSIVE FRACTURE ZONE UNDER PASSIVE CONFINEMENT

Analysis of steel-tube confined concrete columns with increasing steel ratio and slenderness was performed to determine the effect of these parameters on the length of compressive localization zone in concrete. The columns have a cross-section of 130ϕ mm and the investigated heights are 260, 390, and 520 mm. The steel ratios evaluated are 0.9%, 1.80%, 8.0%, and 14.8% representing tube thicknesses of 0.3, 0.6, 2.65, and 5.0 mm, respectively. For all columns, the same RBSM input mesh size is used equal to 12 mm while a 10 mm mesh is used for modeling the steel tube. The concrete strength used is 40 MPa and the yield strength of steel is 250 MPa. The load was applied only to concrete section using as displacement control scheme applied on a rigid top plate. A fixed boundary condition is used for all the analysis.

The axial stress-strain (normalized by the maximum stress) results of analyzed columns are given in Fig. 5. The graphs are group into four in terms of steel ratio. In each graph, results for columns with different slenderness are shown. From these figures, it is clear that for columns with low steel ratio, i.e. 0.9 and 1.8%, the stress-strain diagram is not constant and is a function of the column slenderness. Larger columns tend to have lower ductility than smaller columns. This behavior was reduced using a steel ratio of 8% and completely vanish for steel ratio of 14.8%. Thus, it can be said that for the investigated column slenderness, steel ratios of 8.0% and 14.8% showed a more or less constant stress-strain curve. To further evaluate these results, the localization length of each column was studied by extracting the local axial strain in RBSM.

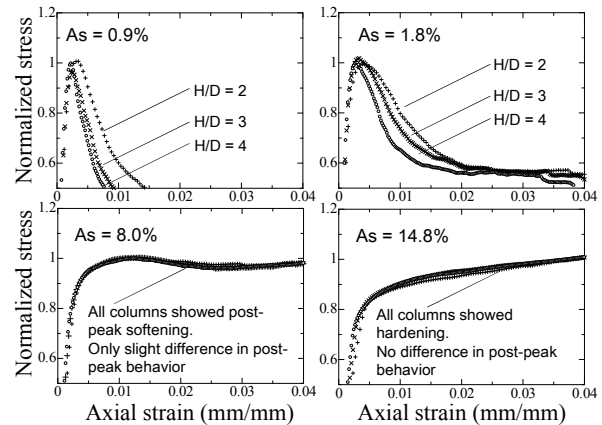


Figure 5 Effect of column slenderness on axial stress-strain curve

Fig. 6 shows the plot of local axial strain in RBSM for each column of different slenderness and arranged in increasing steel ratio. The local axial strains were determined at 40 mm interval. The four plots for each column represent the axial strain at ϵ_{peak} , $2\epsilon_{peak}$, $3\epsilon_{peak}$, and $4\epsilon_{peak}$ for strain softening columns and ϵ_{yield} , $2\epsilon_{yield}$, $4\epsilon_{yield}$, and $6\epsilon_{yield}$ or 0.04 global strain whichever is greater for hardening columns. The zone of localization is defined as the zone where the local axial strain continuously increases, while beyond this zone, the local axial strain decreases. The localization zone is represented by the shaded portion in Fig. 6. Evaluation of the length of compressive fracture zone shows a clear trend for all column slenderness, that is, the length of compressive fracture zone increases with increasing steel ratio. The length of localization zone also corresponds to the simulated damage in concrete and steel tube. For columns with steel ratio of 14.8%, localization of axial strain is not visible for all column slenderness. It is interesting to note that for the case of a column with 8.0% steel ratio, localization of axial strain was not observed for $H/D = 2$ and 3, while when the $H/D = 4$, localization of axial strain can be observed.

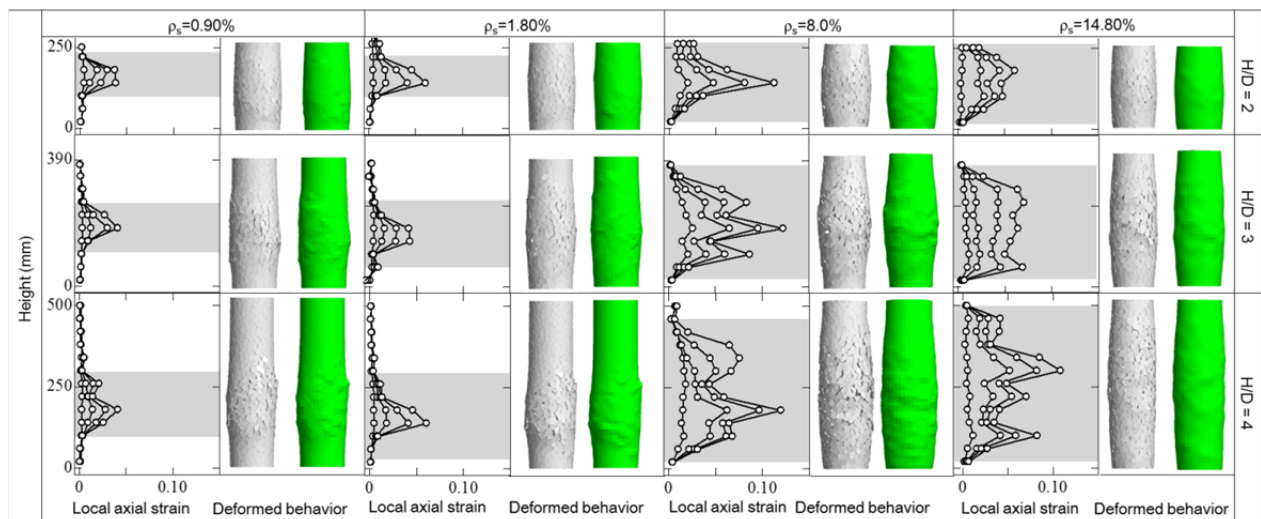


Figure 6 Length of compressive fracture zone for columns with different slenderness and steel ratio.

The development of local axial strain in RBSM and lateral stresses in the steel tube was compared for columns with 1.8% and 8.0% steel ratio and with $H/D = 4$ at different loading stages (expressed in terms of global axial strain) until the load corresponding to the axial strain at peak ϵ_{peak} . The results are shown in Fig. 7. It can be observed that initially, the location of lateral stress concentration are the same for both columns; but as the loading progresses, the stresses for 8% case propagates until it extends on almost the entire column height. For small steel ratio, however, this propagation of lateral stress was not observed and the stresses remain concentrated near mid-height. This observation is consistent with the observed behavior of local axial strain in RBSM. The strains for lower steel ratio column concentrates near mid-height while for the case of a column with 8% steel ratio, the increase in strain is fairly uniform along the height. This means that when the confining pressure provided by steel tube is low, the steel tube is unable to restrain the expansion of concrete and thus concrete deforms laterally and localization of damage occurs. However, when the confining pressure provided by steel is high, the expansion of concrete is prevented and the damage is forced to propagate longitudinally along the member length. This may explain why the length of localization zone increases with increasing confinement as is shown in Fig. 6.

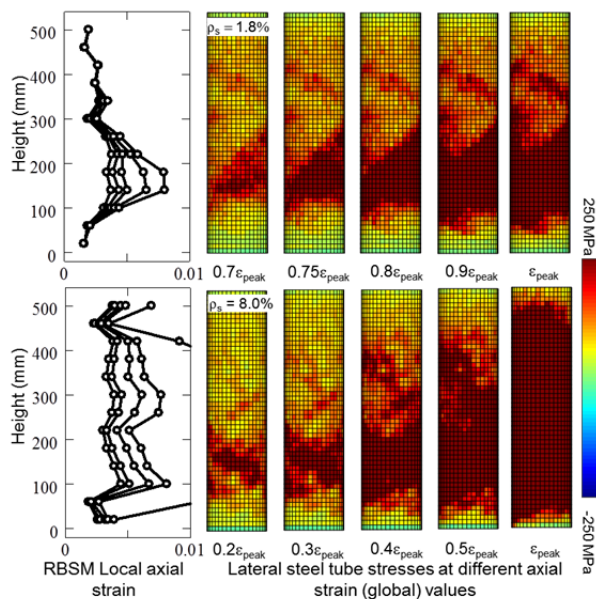


Figure 7 Comparison of lateral steel stress and RBSM local axial strain development for Columns with 1.8% and 8.0% steel ratio.

6. CONCLUSIONS

Based on the presented analysis results, the following are concluded:

- (1) The coupled RBSM-shell model can well simulate the compressive behavior of concrete under steel tube confinement including the expansion of concrete and steel.
- (2) The compressive behavior of steel-tube confined concrete columns is localized. The length of

compressive fracture zone was found to increase with increasing steel ratio. This is because when the confinement provided by steel is low, the steel is unable to restrain the expansion of concrete and localization occurs. However, when the confining pressure provided by steel is sufficient, the steel tube prevents the expansion of concrete and forces the damage to propagate along the length of the member and thus the length of localization zone increases.

- (3) The length of compressive localization zone for columns with 8% steel ratio was not observed for columns with $H/D = 2$ and 3 but was visible for columns with $H/D = 4$. This confirms that the length of localization zone is a function of both column steel ratio and slenderness.

REFERENCES

- [1] Mander, J.B., Priestly, J.N., Park, R., "Theoretical stress-strain model for confined concrete." *J.Struct.Eng.*, 1988, 1804-1826.
- [2] Nakamura, H., Higai, T., "Compressive fracture energy and fracture zone length of concrete. Modeling of Inelastic Behavior of RC Structures under Seismic Loads." ASCE, 2001, 471-487.
- [3] Federation internationale du beton (*fib*), "Practitioners' guide to finite element modeling of reinforced concrete structures." 2008, pp 86-87.
- [4] Caner, F.C., Bazant, Z.P., "Lateral confinement needed to suppress softening of concrete in compression." *J. Eng. Mech.*, 2002, 1304-1313
- [5] Wu, Y., Wei, Y., "Stress-strain modeling of concrete columns with localized failure: An analytical study," *J. Compos. Constr.*, ASCE, 20, 2016.
- [6] Yamamoto, Y., Nakamura, H., Kuroda, I., Furuya, N., "Crack propagation analysis of reinforced concrete wall under cyclic loading using RBSM." *European J. of Civil Eng.* 2014; 18 (7): 780-792
- [7] Mendoza, R.J., Yamamoto, Y., Nakamura, H., Miura, T., "Modeling of localization and softening behavior of passively confined concrete using coupled RBSM and nonlinear shell FEM." *Computational Modeling of Concrete and Concrete Structures*, CRC Press, (In press).
- [8] Mendoza, R.J., Yamamoto, Y., Nakamura, H., Miura, T., "Modeling of composite action in concrete-filled steel tubes using coupled RBSM and shell FEM." *Proc. of the Japan Concrete Institute*, 2017, 39(2): 991-996.
- [9] Lahlou, K., Aitcin, P.C., Chaallal, O., "Behavior of high strength concrete under confined stresses," *Cement & Conc. Comp.*, 12, 1992, 185-193.
- [10] Johansson, M., Gyltoft, K., "Mechanical behaviour of circular steel-concrete composite stub columns." *J. Struct. Eng.* ASCE 2002; 128(8): 1073-1081.
- [11] Nezamian, A., Al-Mahaidi, R., "Bond strength of concrete plugs embedded in tubular steel piles under cyclic loading," *Canadian J. Civil Eng.* 2006, 111-125.